Journal of Electronics, Electromedical Engineering, and Medical Informatics
Homepage: jeeemi.org; Vol 8. 3,July 2026, pp:1148-1162. e-ISSN: 2656-8632

RESEARCH ARTICLE OPEN ACCESS

Design and Mechanical Evaluation of a Polymer Keel SACH Foot Using Finite Element Analysis and Experimental Validation

Agus Setyo Nugroho[1, 2], Kazuhiko Sasaki[1], Muhammad Nouman[1], and Rifky Ismail[3]

[1] Sirindhorn School of Prosthetics and Orthotics, Faculty of Medicine, Siriraj Hospital, Mahidol University, Bangkok, Thailand
[2] Department of Prosthetic and Orthotic, Politeknik Kesehatan Surakarta, Surakarta, Indonesia
[3] Department of Mechanical Engineering, Diponegoro University, Semarang, Indonesia

Corresponding author:Kazuhiko Sasaki (e-mail: kazuhiko.sas@mahidol.edu), **Author(s) Email**: Agus Setyo Nugroho (e-mail: agussetyo.nug@gmail.com) , Muhammad Nouman (e-mail: muhammad.nou@mahidol.ac.th), Rifky Ismail (e-mail: rifky_ismail@ft.undip.ac.id)

Abstract. Conventional Solid Ankle Cushion Heel (SACH) foot commonly uses wooden keels, which may exhibit variability in mechanical properties and limited long-term durability. This study aimed to develop and evaluate a polymer-based keel SACH foot as a low-cost alternative with improved mechanical performance. An integrated methodology combining finite element analysis (FEA) and experimental validation was employed. Three polymer keel SACH foot configurations were designed and analyzed under loading conditions that represent heel strike, mid-stance, and terminal stance, in accordance with ISO 10328. The optimal design was subsequently fabricated and tested under static loading conditions to validate the numerical model. The models utilized ABS for the keel, HDPE for the footplate, and vulcanized rubber for the foot body. Mechanical performance was assessed through total deformation, von Mises stress, strain, and safety factor analysis. Among the three configurations, Model A demonstrated the best mechanical performance, with the lowest average deformation (20.12 mm), the lowest stress concentration (12.67 MPa), and the highest safety factor (1.59). The selected design was subsequently fabricated and validated experimentally under static loading conditions up to 1176.78 N. Experimental validation showed strong agreement with FEA predictions, with deviations below 5% across all gait phases, confirming the accuracy of the FEA model. Comparative testing against a conventional wooden-keel SACH foot revealed significantly lower deformation values for the polymer-based keel SACH foot ($p < 0.05$), indicating improved structural stiffness and more efficient load distribution during loading process. These findings suggest that replacing conventional wooden keels with polymer-based structures can enhance mechanical consistency and structural reliability, while maintaining manufacturability and cost-effectiveness. The proposed design offers a promising approach to developing an affordable and durable prosthetic foot, particularly for use in low- and middle-income countries.

Keywords: SACH foot; polymer keel; finite element analysis; prosthetic foot; mechanical testing; lower limb prosthesis; experimental validation; biomechanical performance.

I. Introduction

Lower-limb amputation remains a major healthcare challenge worldwide, particularly in low- and middle-income countries (LMICs), where access to affordable and durable prosthetic devices remains limited [1][2][3]. Among the available prosthetic foot designs, the Solid Ankle Cushion Heel (SACH) foot remains one of the most widely prescribed options because of its simple non-articulated structure, low maintenance requirements, and low manufacturing cost [2][4]. Originally introduced as a low-maintenance prosthetic solution consisting of a rigid core wrapped in a flexible foam shell [4][5][6], the SACH foot remains widely used in low-resource rehabilitation programs worldwide.

Conventional SACH foot commonly utilizes wooden keels to provide internal structural support and facilitate balance during ambulation [7][8][9]. Although wooden keels are inexpensive and easily sourced, they exhibit severe mechanical limitations, including low flexibility and poor shock-absorption capability [7][8][10]. Wood is highly susceptible to brittle failure and environmental degradation from moisture exposure, which compromises its long-term structural integrity and leads to unpredictable performance variations [9][11]. Furthermore, traditional wooden-keel SACH foot lacks

Manuscript received 8 May *2026*; Revised 10 June *2026*; Accepted 21 June *2026*; Available online 12 July *2026*
Digital Object Identifier (**DOI**): https://doi.org/10.35882/jeeemi.v8i3.1807

the energy storage and return (ESR) characteristics found in modern prosthetic foot, limiting their suitability for users with higher mobility demands [7].

To overcome these mechanical deficiencies, several studies have investigated alternative materials, particularly carbon fiber-reinforced polymers (CFRP) and advanced hybrid composite structures. Previous research has demonstrated that CFRP-based prosthetic foot provides exceptional fatigue life, higher energy return, and enhanced biomechanical performance compared with traditional wooden designs [12][13]. However, the superior performance of CFRP system is accompanied by high material costs and greater manufacturing complexity, which significantly limit their practical adoption in resource-constrained environments [12].

To bridge the gap between fragile wooden keels and cost-prohibitive CFRP alternatives, affordable thermoplastic polymers such as ABS and HDPE have emerged as potential alternatives [15][16][17]. Nevertheless, the existing studies on these affordable polymers predominantly focus on non-prosthetic applications [18][19][20], leaving the structural behavior, deformation characteristics, and load-bearing performance of fully polymer-based keel SACH foot insufficiently understood and lacking robust experimental validation [14][21]. Resolving this research gap is of paramount importance for LMIC prosthetic services, as understanding these mechanical properties directly dictates the device's mechanical reliability under repetitive gait cycles, ensures consistent manufacturability using affordable local techniques, and fosters long-term clinical adoption by providing amputees with a highly reliable, durable, and predictable prosthetic solution. Finite element analysis (FEA), paired with comprehensive experimental cross-examination, serves as an essential framework for achieving this structural optimization before physical deployment [14][21][22][23].

To address these requirements, this study aims to design, evaluate, and experimentally validate a polymer-based keel SACH foot as a low-cost alternative, and to assess its mechanical performance relative to a conventional wooden-keel design under ISO 10328-standardized loading conditions. The technical novelty and primary contribution of this study lie in the synergistic material combination of an ABS keel, an HDPE footplate, and a vulcanized rubber cover, coupled with a continuous reinforced keel geometry specifically optimized for low-cost manufacturing. Furthermore, this study establishes a highly robust validation protocol that integrates exact numerical predictions with quasi-static mechanical testing. To position this novelty sharply, the proposed design addresses critical gaps left by recent prosthetic foot studies. For instance, while studies by Vasanthanathan et al. [21] and Balaramakrishnan et al. [23] utilized expensive carbon fiber-reinforced polymers (CFRP) that exhibited high peak stresses, the proposed ABS-HDPE architecture significantly reduces material costs while maintaining a highly competitive maximum deformation (36.22 mm) and a secure safety factor (1.59). Moreover, compared with the conventional and composite SACH foot models analyzed by Omasta et al. [22] and Worajinda et al. [14] which reported numerical-experimental validation errors ranging from 15.22% to 30%, this study demonstrates vastly superior validation accuracy, with an error margin of less than 5%. Finally, unlike studies that focus solely on non-prosthetic polymer applications [18][19], this research presents a direct, quantitative mechanical comparison between the optimized polymer keel and a commercially available wooden-keel SACH foot, demonstrating the keel's viability for broad clinical adoption in LMICs.

II. Method

A. Research Workflow

The overall methodology of this study is structured into two main phases: numerical simulation and experimental validation. The complete procedural flow, from initial material selection to the final comparative analysis against a conventional wooden-keel SACH foot, is illustrated in Fig. 1.

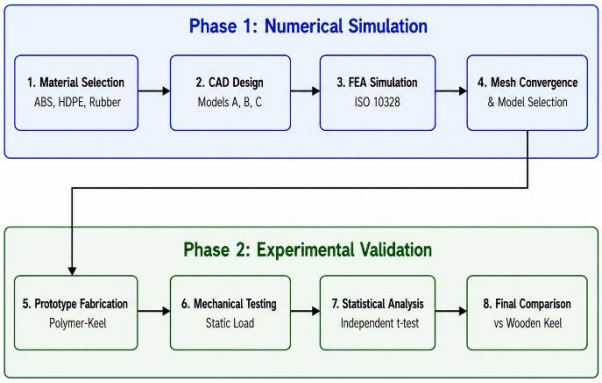

Fig. 1. Block diagram of the research workflow.

As illustrated in Fig. 1, the research methodology follows a structured, sequential framework divided into two primary phases: computational simulation and experimental validation. The first phase began with material characterization and selection, in which the precise mechanical properties of ABS, HDPE, and vulcanized rubber were defined. These parameters were then integrated into three distinct three-dimensional CAD configurations (Models A, B, and C) to investigate geometric effects on structural performance. Finite element analysis (FEA) was

Manuscript received 8 May *2026*; Revised 10 June *2026*; Accepted 21 June *2026*; Available online 12 July *2026*
Digital Object Identifier (**DOI**): https://doi.org/10.35882/jeeemi.v8i3.1807

subsequently executed under standardized ISO 10328 loading conditions, accompanied by a rigorous mesh convergence study to ensure numerical independence and select the optimal configuration (Model A). In the second phase, the optimized design was physically translated through prototype fabrication and subjected to static mechanical testing up to 1176.78 N across three crucial gait phases (heel strike, mid-stance, and terminal stance). Finally, an independent-samples t-test and Cohen's d effect-size analysis were conducted to provide a robust, quantitative biomechanical evaluation that directly compares the polymer-keel prototype with a conventional wooden-keel SACH foot.

B. Experimental Design

In this study, a comparative experimental study design was used. This study has the following objectives: (1) to validate the results of the FEA simulation with real conditions and (2) to compare the mechanical test results on the SACH foot prototype with the local SACH foot available in Indonesia. The SACH foot prototype, developed based on FEA simulation results, has been validated through real-world mechanical testing under the same boundary conditions as the FEA simulation. The boundary conditions for assessing the prosthetic SACH foot model comply with the ISO 10328 standard used in this study. This condition was applied to three key points in the stance phase of the walking cycle: (i) heel strike, (ii) mid-stance, and (iii) terminal stance. During heel strike, the SACH prosthetic foot model was positioned at a 15° slope towards back flexion relative to the fulcrum plane. In mid-stance, the model was neutral, perpendicular to the fulcrum plane. In the terminal stance, the model position involves a 20° tilt towards plantar flexion relative to the stalk plane [25].

As shown in Fig. 2 and Table 1, a fixed support was applied to the SACH foot connector, and a load of 1176.78 N was applied along the Y-axis. During the simulation, the material properties for the Prototype SACH foot were entered. Regarding the material used to make the ABS keel, the foot plate was made of HDPE, and the body cover of the SACH foot was VR, as per Table 2. The total deformation was assessed to validate the FEA simulation results against those from the mechanical test for the SACH foot prototype. The total deformation value is the metric used to validate the FEA simulation results against mechanical test results for the SACH foot prototype. In the deformation testing phase of the SACH Prototype foot compared to the Local SACH foot in Indonesia, a laboratory experimental research method with a static test approach was used to compare the total deformation value between the polymer SACH foot keel prototype and the local SACH foot keel in three gait cycle phases, namely heel strike, middle position, and terminal position. The study used only a post-test group design, in which each SACH foot type was tested under a static load to measure deformation. The research sample consisted of two types of SACH foot: the SACH polymer keel prototype and the SACH local wood keel leg. Each type of SACH foot had five samples, and each was tested with a run pressure test per phase using loads ranging from 0 to 120 Kg (1176.78N) to obtain reliable data.

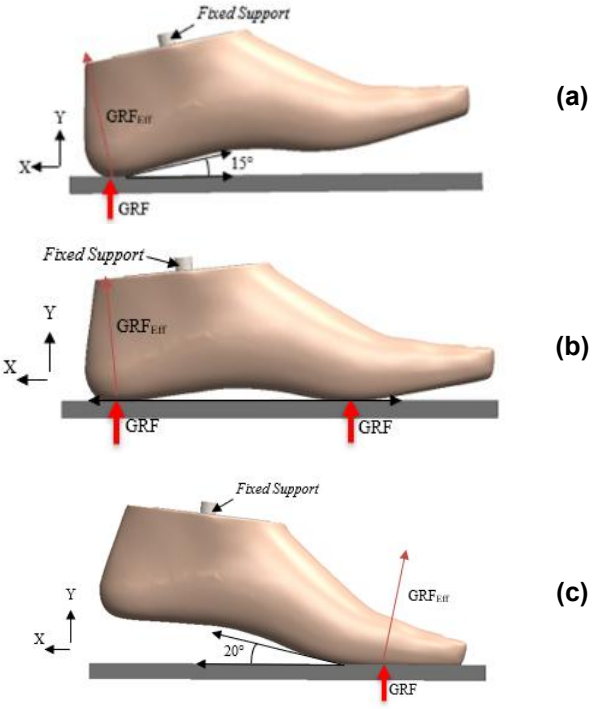

Fig. 2. Boundary conditions (a) Heel Strike, (b) Mid Stance, (c) Terminal Stance.

Table 1. Position and distributed load during simulation.

Loading	Fixed support	Distributed load	Y-axis load
HS	Connector foot	The heel part of the SACH foot	1176.78 N
MS	Connector foot	The heel part and the front third of the SACH foot are connected with support	1176.78 N
TS	Connector foot	The bottom front third of the SACH foot is connected to the support	1176.78 N

Manuscript received 8 May *2026*; Revised 10 June *2026*; Accepted 21 June *2026*; Available online 12 July *2026*
Digital Object Identifier (**DOI**): https://doi.org/10.35882/jeeemi.v8i3.1807

Table 2. Material properties of ABS, HDPE, and VR.

SACH foot component	Materials	Density (Kg/m³)	Young's Modulus (MPa)	Poisson's Ratio	Yield Strength (MPa)	Ultimate Tensile Strength (MPa)
Keel	ABS	1040	324	0.37	40	45
Footplate	HDPE	950	232.66	0.43	26	31
Body cover	VR	1150	18	0.49	-	25

C. SACH Foot Design Configuration

Three SACH foot configurations (Model A, B, and C) were developed and evaluated in this study. All models shared identical external dimensions and material composition, while variations were introduced in the keel geometry and reinforcement arrangement to investigate their influence on structural performance. Fig. 3 illustrates the geometric configurations of the three proposed models.

Model A employed a continuous reinforced keel extending from the heel to the forefoot region to promote uniform load transfer and improve structural stiffness. Model B incorporated reduced keel reinforcement and a supporting footplate structure to increase flexibility under load. Model C used a simplified keel geometry with a smaller cross-section to evaluate the effect of material reduction on mechanical behaviour. The three configurations were analyzed under identical finite element and experimental loading conditions. Their performance was compared based on total deformation, equivalent strain, von Mises stress, and factor of safety to identify the most mechanically efficient design.

To ensure reproducibility and provide a transparent overview of the optimization process, the exact dimensional parameters and total mass of each evaluated configuration are detailed in Table 3. While the overall external dimensions (total length of 240 mm and width of 75 mm) were kept constant to fit a standard prosthetic shell, the internal keel geometries and resulting masses were varied.

Fig. 3. SACH foot design (a) Model A, (b) Model B, (c) Model C.

Table 3. Geometry of SACH Foot Designs A, B, and C

Design	Keel Length	Keel Thickness	SACH Foot Thickness	Foot Plate Length	SACH Foot Length	Foot Plate Thickness	Keel & Foot Plate Mass	SACH Foot Mass
Design A	156 mm	68 mm	75 mm	205 mm	240 mm	3 mm	366.08 g	746.87 g
Design B	121 mm	60 mm	75 mm	205 mm	240 mm	3 mm	351.03 g	731.82 g
Design C	127 mm	62 mm	75 mm	205 mm	240 mm	3 mm	357.06 g	737.85 g

D. Theoretical Formulation

To accurately evaluate the structural behavior of the proposed SACH foot designs under ISO 10328 loading conditions, the finite element analysis relied on a set of governing equations encompassing linear isotropic elasticity, failure criteria, and statistical evaluation. The fundamental behaviour of the finite element model was governed by the global static equilibrium equation, defining the relationship between the global stiffness matrix [K], the nodal displacement vector {U}, and the applied force vector {F} [26]:

$$[K]\{U\} = \{F\} \quad (1)$$

The generalized stress-strain relationship for the homogeneous, isotropic, and linearly elastic polymer materials (ABS and HDPE) was governed by Hooke's Law, expressed in matrix form as [26]:

$$\{\sigma\} = [D]\{\epsilon\} \quad (2)$$

where [D] is the material stiffness matrix. The three-dimensional normal stresses $(\sigma_x, \sigma_y, \sigma_z)$ were calculated based on the elastic modulus (E) and Poisson's ratio (v) [26]:

$$\sigma_x = \frac{E}{(1+v)(1-2v)}\left[(1-v)\epsilon_x + v(\epsilon_y + \epsilon_z)\right] \quad (3)$$

$$\sigma_y = \frac{E}{(1+v)(1-2v)}\left[(1-v)\epsilon_y + v(\epsilon_x + \epsilon_z)\right] \quad (4)$$

$$\sigma_z = \frac{E}{(1+v)(1-2v)}\left[(1-v)\epsilon_z + v(\epsilon_x + \epsilon_y)\right] \quad (5)$$

The shear stresses $(\tau_{xy}, \tau_{yz}, \tau_{zx})$ relate to the shear strains $(\gamma_{xy}, \gamma_{yz}, \gamma_{zx})$ through the shear modulus (G) [26]:

$$\tau_{xy} = G\gamma_{xy}\ ;\ \tau_{yz} = G\gamma_{yz}\ ;\ \tau_{zx} = G\gamma_{zx} \quad (6)$$

Manuscript received 8 May 2026; Revised 10 June 2026; Accepted 21 June 2026; Available online 12 July 2026
Digital Object Identifier (DOI): https://doi.org/10.35882/jeeemi.v8i3.1807

The shear modulus (G) is intrinsically linked to the elastic modulus and Poisson's ratio [26]:

$$G = \frac{E}{2(1+\nu)} \quad (7)$$

Strain-displacement kinematic relationships define how the structural body deforms. The normal strains $(\epsilon_x, \epsilon_y, \epsilon_z)$ along the primary axes are derived from the partial derivatives of displacements (u, v, w) [27]:

$$\epsilon_x = \frac{\partial u}{\partial x}, \epsilon_y = \frac{\partial v}{\partial y}, \epsilon_z = \frac{\partial w}{\partial z} \quad (8)$$

Similarly, the shear strains are expressed as [27]:

$$\gamma_{xy} = \frac{\partial u}{\partial x} + \frac{\partial v}{\partial y}, \gamma_{yz} = \frac{\partial v}{\partial z} + \frac{\partial w}{\partial y}, \gamma_{zx} = \frac{\partial w}{\partial x} + \frac{\partial u}{\partial z} \quad (9)$$

The total magnitude of deformation (U_{total}) at any given node is the vector sum of its directional displacements [27]:

$$U_{total} = \sqrt{u^2 + v^2 + w^2} \quad (10)$$

To evaluate the structural integrity and predict material yielding, the equivalent von Mises stress (σ_{vM}) was utilized, which is highly appropriate for ductile polymers [27]:

$$\sigma_{vM} = \sqrt{\frac{1}{2}[(\sigma_x - \sigma_y)^2 + (\sigma_y - \sigma_z)^2 + (\sigma_z - \sigma_x)^2 + 6(\tau_{xy}{}^2 + \tau_{yz}{}^2 + \tau_{zx}{}^2)]} \quad (11)$$

The Factor of Safety (SF) was evaluated by comparing the material's yield strength (σ_{yield}) against the maximum observed von Mises stress [27]:

$$SF = \frac{\sigma_{yield}}{\sigma_{vM}} \quad (12)$$

For experimental validation, the percentage error (%Error) was calculated to verify the numerical model's reliability against the experimental deformation (δ_{Exp}) and FEA deformation (δ_{FEA}) [27]:

$$\%Error = \left|\frac{\delta_{Exp} - \delta_{FEA}}{\delta_{Exp}}\right| x\ 100\% \quad (13)$$

In the subsequent experimental evaluation, differences between the prototype and local SACH foot were quantified using Cohen's d effect size, relying on the sample means $(\overline{x_1}, \overline{x_2})$ and pooled standard deviation (s_{pooled}) [27]:

$$d = \frac{\overline{x_1} - \overline{x_2}}{s_{pooled}} \quad (14)$$

In the aforementioned formulations, [K] represents the global stiffness matrix (N/mm), {U} is the nodal displacement vector (mm), and {F} is the applied force vector (N). Within the material stiffness matrix [D], the parameters E and G denote the elastic and shear moduli (MPa), respectively, while ν represents the dimensionless Poisson's ratio. The normal stresses $(\sigma_x, \sigma_y, \sigma_z)$ and shear stresses $(\tau_{xy}, \tau_{yz}, \tau_{zx})$ are expressed in MPa, corresponding to the directional normal strains $(\epsilon_x, \epsilon_y, \epsilon_z)$ and shear strains $(\gamma_{xy}, \gamma_{yz}, \gamma_{zx})$ which are dimensionless (mm/mm). Furthermore, U_{total} indicates the global deformation magnitude (mm), and the equivalent von Mises stress σ_{vM} (MPa) serves as the primary metric for predicting ductile polymer yielding against the material's limit σ_{yield} (MPa).

E. Finite Element Analysis Setup

Finite element analysis (FEA) was performed using ANSYS Workbench 2019 R3 (ANSYS Inc., USA) to evaluate the structural performance of the proposed SACH foot designs. Three-dimensional CAD models were imported into the static structural module and assigned material properties corresponding to ABS, HDPE, and vulcanized rubber, as summarized in Table 2. All materials were assumed to be homogeneous, isotropic, and linearly elastic. The models were discretized using second-order tetrahedral elements (SOLID 187). A mesh convergence study was conducted by varying the global element size from 3.0 mm to 0.5 mm. The final mesh size of 1.0 mm was selected when the variation in maximum von Mises stress between successive refinements was less than 5%, resulting in an extremely fine and optimal mesh with 5,985,670 elements and 8,337,986 nodes. Mesh quality was strictly verified, ensuring an average element quality above 0.85 and skewness below 0.25 to prevent numerical stiffening. Bonded contact assumptions were applied at all material interfaces (ABS keel, HDPE footplate, and vulcanized rubber), assuming perfect adhesion without relative sliding or separation under load.

Furthermore, a linear elastic assumption was justified for all materials because the preliminary analysis indicated that the maximum induced stresses remained well below the respective yield strengths, and the structural deformations were geometrically small relative to the overall dimensions. The connector region was constrained using a fixed-support boundary condition to represent attachment to the prosthetic pylon. Loading conditions were established in accordance with ISO 10328 and consisted of heel strike (15° dorsiflexion), mid-stance (0°), and terminal stance (20° plantarflexion). Loading conditions were established using an adapted quasi-static protocol guided by ISO 10328 structural testing principles. A static vertical load of 1176.78 N was specifically applied to represent a maximum user body mass of 120 kg. This specific load threshold was selected to match the heavy-duty weight limit commonly adopted by commercial imported prosthetic foot, ensuring the prototype's structural reliability for heavier amputees. The analyses were performed using a linear static solver. Total deformation, equivalent strain, von Mises stress, and factor of safety were evaluated to compare the structural performance of the three SACH foot configurations. The factor of safety was calculated using the von Mises failure criterion implemented in ANSYS Workbench 2019 R3. Numerical results were subsequently validated through experimental mechanical testing under equivalent loading

Manuscript received 8 May *2026*; Revised 10 June *2026*; Accepted 21 June *2026*; Available online 12 July *2026*
Digital Object Identifier (**DOI**): https://doi.org/10.35882/jeeemi.v8i3.1807

conditions. To evaluate the accuracy of the numerical model, the percentage deviation between finite element predictions and experimental measurements was calculated. Based on commonly accepted validation practices in biomechanical and engineering finite element studies, deviations below 5% were considered indicative of excellent agreement, while deviations below 10% were considered acceptable for complex biomechanical structures and material systems. Similar validation criteria have been adopted in previous prosthetic and biomedical finite-element investigations [23][14]. The computational procedure for the FEA and validation process followed a systematic algorithm to ensure reliability:

1. Input

The 3D CAD geometries (Models A, B, C) was imported into ANSYS. Define material properties (Young's modulus, Poisson's ratio, density) for ABS, HDPE, and Vulcanized Rubber.

2. Meshing

The initial mesh was generated using SOLID187 elements. The mesh convergence study iteratively (reducing element size from 3.0 mm to 1.0 mm) was performed until maximum stress variation is <5 %.

3. Boundary Conditions and Loading

The bonded contacts between components was applied. Then, the pylon connector was fixed. Furthermore, 1176.78 N vertical ground reaction force was applied under three phases: Heel Strike (15° dorsiflexion), Mid-Stance (0°), and Terminal Stance (20° plantarflexion).

4. Execution

The linear static equations was solved to extract output parameters (Total Deformation, Equivalent Strain, von Mises Stress, Safety Factor).

5. Decision-Making

The outputs across models was compared. Then, the optimal configuration was selected based on the lowest deformation, minimum stress concentration, and SF > 1.0.

6. Validation

The selected model's FEA deformation was compared with the experimental data. If the percentage error is <5 %, the model is considered valid; otherwise, the material and contact assumptions needs to be recalibrated.

F. Mechanical Testing Procedure

Experimental validation was conducted using a calibrated Zwick Roell Z020 universal testing machine (ZwickRoell GmbH & Co, Germany) with a load capacity of 20 kN. Machine calibration was verified in accordance with ISO 7500-1 prior to testing. Five specimens were tested for each prosthetic foot type (Polymer-keel and wooden-keel SACH foot), for a total of 10 specimens, as shown in Fig. 4. Each specimen was tested three times at each gait-phase position (heel strike, mid-stance, and terminal stance), and the average deformation was reported. Before formal testing, all specimens underwent three preconditioning cycles at 10% of the maximum load to minimize viscoelastic effects. Static loading was applied at a constant crosshead displacement rate of 5 mm/min until the target load of 1176.78 N was reached. Custom steel fixtures were fabricated to replicate the loading orientations specified in ISO 10328. The heel strike test was performed at 15° dorsiflexion, mid-stance at 0°, and terminal stance at 20° plantarflexion, as shown in Fig. 5.

G. Statistical Analysis

Statistical analysis was performed using IBM SPSS Statistics version 29.0. It is important to clarify that the experimental unit in this study uses a repeated-measures design rather than multiple independent specimens. A single prototype SACH foot and a single local wooden-keel SACH foot were each subjected to 5 repeated testing trials (N=5 trials per position) to strictly evaluate the consistency, precision, and repeatability of the mechanical response under machine loading. Since the variance within these repeated trials represents instrument precision rather

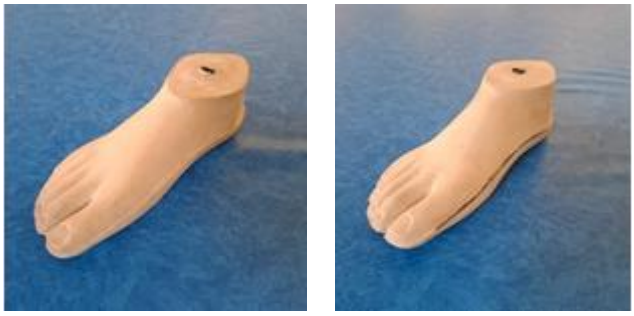

(a) (b)

Fig. 4. SACH foot type for mechanical test: (a) Prototype SACH foot, (b) Local Indonesian SACH foot.

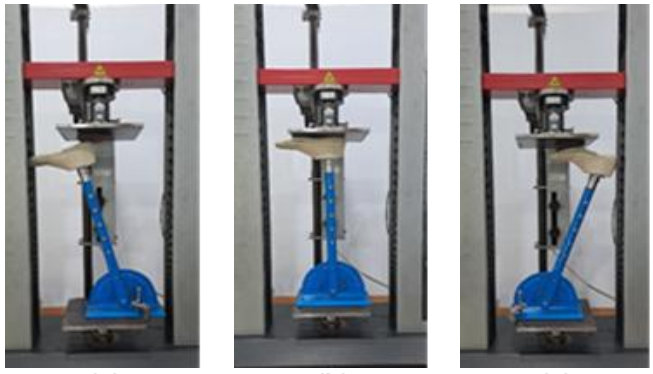

(a) (b) (c)

Fig. 5. Mechanical testing positions: (a) Heel Strike, (b) Mid Stance, (c) Terminal Stance.

Manuscript received 8 May *2026*; Revised 10 June *2026*; Accepted 21 June *2026*; Available online 12 July *2026*
Digital Object Identifier (**DOI**): https://doi.org/10.35882/jeeemi.v8i3.1807

than population variability, standard deviations were exceptionally small. Consequently, instead of a traditional independent t-test, descriptive statistics (Mean and Standard Deviation) were primarily used to plot the data distribution and assess stability. The observed effect sizes (Cohen's d) were reported solely to quantify the absolute mechanical difference between the two configurations under highly controlled laboratory conditions, acknowledging that the massive effect sizes represent machine-level precision differences rather than clinical population variance.

III. Result

A. Finite Element Analysis

The simulation results showed that SACH foot model A was selected over the other two designs. The SACH foot model A has an average total deformation of 20.119 mm, which is 28.99% lower than model B and 22.31% lower than model C. A lower total deformation indicates better material strength and structural performance, meaning that the SACH foot model A has greater resistance under a maximum load of 120 kg (1176.78 N). Additionally, the SACH foot model A has an average maximum von Mises stress of 12.670 MPa, which is significantly lower compared to 38.718 MPa for the SACH foot model B and 79.667 MPa for the SACH foot model C. It suggests that the SACH foot model A exhibits the lowest maximum von Mises stress among the materials used in its manufacture, namely ABS, HDPE, and Vulcanized Rubber. The strain value for the SACH foot model A is also the smallest, at 0.101.

The minimum factor of safety obtained for Model A was 1.59, indicating that the maximum von Mises stress remained below the yield strength of the ABS keel material under all loading conditions. Since failure initiation was governed by the most highly stressed region, the minimum factor of safety was considered the primary design acceptability criterion rather than the average factor of safety. The numerical results explicitly demonstrate why Model A performs biomechanically better than Models B and C. The superior performance of Model A is fundamentally attributed to its continuously reinforced keel geometry that extends from the heel to the forefoot. This continuous structural volume allows the 1176.78 N ground reaction force to be distributed evenly across a larger surface area, effectively preventing localized stress concentrations. In contrast, the reduced keel reinforcement in Model B and the simplified, smaller cross-section in Model C fail to disperse the mechanical load efficiently. Consequently, Models B and C suffer from significantly higher localized von Mises stress (38.71 MPa and 79.66 MPa, respectively) and excessive deformation. Fig. 6 visually confirms this structural trend, showing that Model A maintains the lowest median values and the tightest variance across all critical metrics (deformation, stress, strain, and safety factor), thereby establishing it as the most structurally robust configuration and the recommended choice for further development.

Although the minimum factor of safety 1.59 is lower than values commonly adopted in highly conservative structural engineering applications, it remains above unity and indicates that the design can safely withstand the prescribed ISO 10328 static loading condition without material yielding. Similar safety factor ranges have been reported in preliminary prosthetic foot development studies, where structural efficiency, weight reduction, and flexibility must be balanced against mechanical strength. Mechanical testing should now be conducted to validate the FEA results and confirm the suitability of the SACH foot model A for production.

B. Validation with Mechanical Testing of Prototype SACH Foot

The mechanical test results indicated that the prototype SACH foot exhibited total deformation within the

Table 4. Comparison of total deformation results of FEA with Mechanical Test.

Total deformation prototype SACH foot model A			
Positions	**FEA**	**Mechanical Test**	**% difference**
HS	17.825 mm	17.08 mm	4.18
MS	5.263 mm	5.22 mm	0.81
TS	37.269 mm	36.22 mm	2.81

Table 5. Results of the mechanical comparison of the SACH foot test.

Position	Mean Prototype ± SD (mm)	Mean Local ± SD (mm)	Mean Difference (mm)	p-value	Cohen's d (within-instrument)	95% CI (Lower-Upper)
Heel Strike	17.10 ± 0.026	18.15 ± 0.018	1.052	< 0.001	47.77	1.020 – 1.084
Mid Stance	5.21 ± 0.026	5.83 ± 0.023	0.620	< 0.001	25.42	0.584 – 0.656
Terminal Stance	36.07 ± 0.460	37.19 ± 0.019	1.122	0.0054	3.45	0.647- 1.597

Cohen's d reflects instrument precision, not clinical effect size.

Manuscript received 8 May *2026*; Revised 10 June *2026*; Accepted 21 June *2026*; Available online 12 July *2026*
Digital Object Identifier (**DOI**): https://doi.org/10.35882/jeeemi.v8i3.1807

(a)

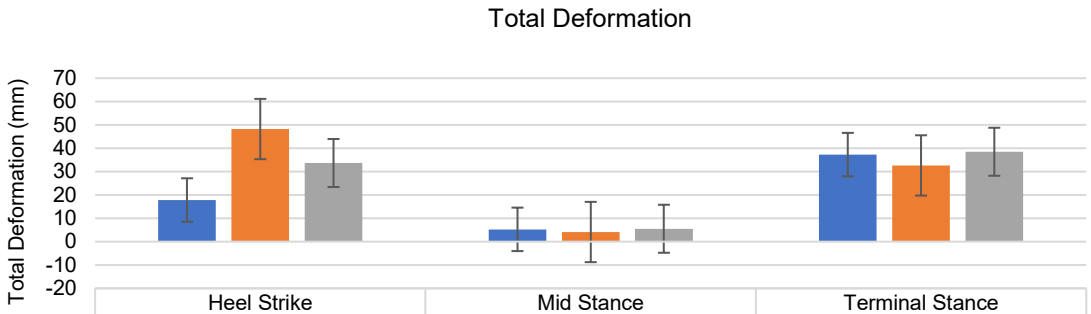

	Heel Strike	Mid Stance	Terminal Stance
SACH foot model A	17.825	5.2625	37.269
SACH foot model B	48.234	4.1271	32.641
SACH foot model C	33.67	5.521	38.496

(b)

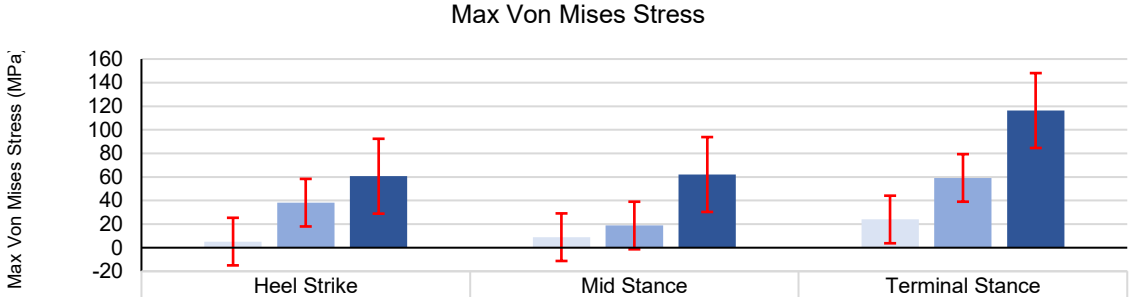

	Heel Strike	Mid Stance	Terminal Stance
SACH foot model A	5.1732	8.9095	23.928
SACH foot model B	38.17	18.821	59.162
SACH foot model C	60.61	62.072	116.32

(c)

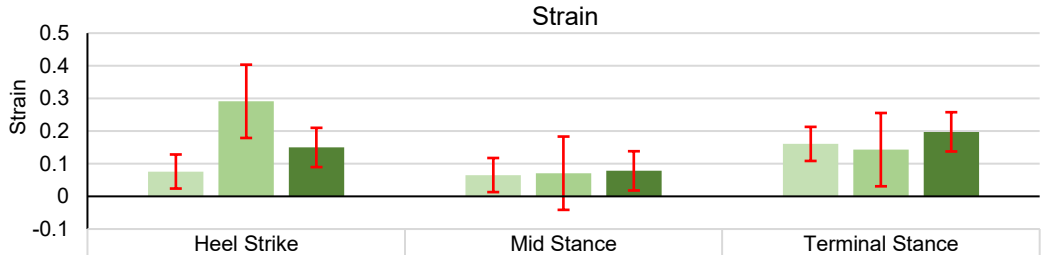

	Heel Strike	Mid Stance	Terminal Stance
SACH foot model A	0.076102	0.06529	0.16065
SACH foot model B	0.29114	0.0709	0.14312
SACH foot model C	0.14978	0.078164	0.19765

(d)

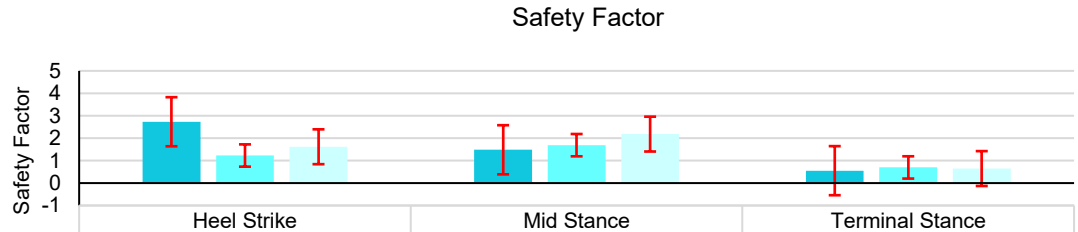

	Heel Strike	Mid Stance	Terminal Stance
SACH foot model A	2.7333	1.4841	0.55263
SACH foot model B	1.228	1.69	0.69717
SACH foot model C	1.6189	2.1828	0.64754

Fig. 6. The boxplot of FEA results for up to three SACH foot designs: (a) Total Deformation, (b) Max von Mises Stress, (c) Strain, and (d) Safety Factor.

Manuscript received 8 May *2026*; Revised 10 June *2026*; Accepted 21 June *2026*; Available online 12 July *2026*
Digital Object Identifier (**DOI**): https://doi.org/10.35882/jeeemi.v8i3.1807

acceptable range, consistent with the FEA simulation results. At heel strike, the prototype exhibited a total deformation of 17.08 mm, which was 4.18% lower than the FEA predictions. During mid-stance, the total deformation measured was 5.22 mm, which is 0.81% lower than the FEA results. At the terminal stance, the deformation was 36.22 mm, 2.81% lower than the FEA simulation. These findings confirm that the difference between the FEA and mechanical tests is less than 5%, validating both methods. As shown in **Table 4**.

C. Mechanical Testing: Prototype SACH foot and Local SACH foot

Prior to comparative analysis, the assumptions of normality and homogeneity of variance were evaluated. The Shapiro-Wilk test indicated that deformation data at all loading positions were normally distributed ($p > 0.05$), while Levene's test confirmed homogeneity of variance between groups ($p > 0.05$). Therefore, an independent samples t-test was considered appropriate for subsequent analyses. At the heel strike position, the independent sample t-test revealed a statistically significant difference in total deformation between the prototype and local SACH foot ($t(8) = 75.53$, $p<0.001$). The mean difference is 1.052 mm, with a 95% confidence interval ranging from 1.020 mm to 1.084 mm. Since the confidence interval does not cross zero, the difference can be considered statistically reliable. These findings demonstrate that the prototype SACH foot exhibited lower deformation and greater structural rigidity during heel-strike loading. At the mid-stance position, a significant difference was also observed between the two SACH foot designs ($t(8) = 40.19$, $p < 0.001$). The mean difference in deformation is 0.620 mm, with a 95% confidence interval that excludes zero, confirming the robustness of the observed difference. The calculated effect size indicated a large practical effect, suggesting that the prototype SACH foot maintains superior structural stiffness during mid-stance loading. At the terminal stance position, the independent-samples t-test also showed a significant difference between the prototype and the local SACH foot ($t(8) = 5.45$, $p = 0.0054$). The mean difference is 1.122 mm, with a 95% confidence interval ranging from 0.647 mm to 1.597 mm. Since the confidence interval remained entirely above zero, the difference was considered statistically meaningful. Furthermore, the observed effect size indicated a large practical effect. The significance level remained below the Bonferroni-adjusted threshold ($p < 0.017$), confirming that the results were robust even after correction for multiple comparisons. As shown in Table 5. Effect size analysis showed very large and large differences between the prototype and the local SACH foot across all loading positions. These values indicate that the observed deformation differences are not only statistically significant but also practically substantial.

IV. Discussion

A. Design Performance and Structural Behavior

The results of the finite element analysis (FEA) show that the variety of SACH foot designs significantly influenced the mechanical response, specifically deformation, stress distribution, strain, and safety factors. Model A consistently showed the best performance, indicating that its geometric configuration optimized load distribution during gait compared with Models B and C. The lower total deformation in Model A indicated greater structural rigidity, an important parameter in the design of a prosthetic foot. In the latest literature, stiffness optimization is a key factor in improving stability and energy efficiency during walking [28]. Prosthetic foot deformation tends to increase significantly during the terminal stance phase, and a design that limits excessive deformation will result in more stable gait performance [29]. This is consistent with the results of this study, in which Model A exhibited the lowest deformation, potentially improving postural control and user comfort. The lower von Mises stress distribution in Model A indicates the design's ability to minimize local stress concentrations. This phenomenon is particularly important because stress concentration is a major factor in material failure in prosthetic components. Maximum stress in prosthetic foot structures is typically localized to specific areas, such as the heel or midfoot, which are critical failure points [23]. Thus, the low maximum stress in Model A suggests that this design is more effective in evenly distributing the load and reducing the risk of structural failure. In addition, the lower strain value in Model A indicates that the material works within safe elastic limits. In the context of biomechanics, this is important to maintain structural integrity during long-term use. Recent studies show that strain analysis via FEA can be used to evaluate the durability and reliability of prosthetic designs before experimental testing [22].

Thus, these results indicate that Model A has a longer potential service life than other models. The higher safety factor in Model A also reinforces the finding that this design is more resistant to extreme load conditions. From a design perspective, the minimum factor of safety is generally considered more critical than the average factor of safety because structural failure typically initiates in local regions of highest stress concentration. Therefore, the minimum factor of safety provides a more conservative and reliable indicator of structural integrity for prosthetic applications. The minimum factor of safety of 0.533 obtained for Model A indicates that the design has an adequate safety margin under the investigated loading conditions while maintaining acceptable structural

Manuscript received 8 May *2026*; Revised 10 June *2026*; Accepted 21 June *2026*; Available online 12 July *2026*
Digital Object Identifier (**DOI**): https://doi.org/10.35882/jeeemi.v8i3.1807

efficiency. In prosthetic foot design, excessively high safety factors are not always desirable because they may increase structural stiffness and weight, potentially reducing flexibility and energy-storage capability. Therefore, the observed safety factor represents a practical compromise between mechanical safety and functional performance. It should be noted that prosthetic foot structures are typically designed to balance strength, weight, flexibility, and energy-storage characteristics. Consequently, excessively high safety factors are not always desirable, as they may increase structural stiffness and material use without necessarily improving the functional performance. Therefore, the observed factor of safety of 1.59 may be considered acceptable for the present static-loading evaluation, although future fatigue and cyclic–loading studies are required to further establish long-term structural reliability. In modern prosthetic designs, safety factors account for not only static loads but also cyclic loads encountered during daily activities. The evaluation of safety factors using FEA is essential for optimizing the strength-to-weight ratio and ensuring structural reliability under repeated load cycles [30].

Interestingly, all models exhibit the highest deformation and stress values during the terminal stance phase. These findings are consistent with recent research showing that the terminal stance phase is critical in the gait cycle due to maximum energy transfer and the highest ground reaction force [31]. Therefore, Model A's ability to maintain optimal performance in this phase suggests that its design is more adaptive to extreme load conditions. From a design perspective, these results also confirm that geometry optimization plays a more dominant role than material selection alone. A non-linear FEA approach that accounts for geometry, materials, and contact interactions can provide more accurate biomechanical predictions and aid in the development of more efficient prosthetic designs [29]. In addition, the use of a combination of materials such as ABS, HDPE, and rubber aligns with recent trends in prosthetic design that combine structural rigidity with energy-absorption capabilities [32][33]. Recent studies have shown that integrating elastomeric materials, such as rubber, can improve energy return and gait adaptation [34].

To fully contextualize the mechanical viability of the proposed polymer-keel SACH foot, the numerical findings of Model A were directly compared with specific values from previous prosthetic foot studies. When evaluated against the conventional prosthetic foot analyzed by Omasta et al. [22], which reported a maximum total deformation of 37.22 mm, our Model A exhibits a lower peak deformation of 36.22 mm at terminal stance, indicating improved structural rigidity despite using lower-cost polymer materials. Regarding stress distribution, the maximum von Mises stress of 12.67 MPa in our ABS-based keel is drastically lower than the 490.76 MPa peak compressive stress reported in the CFRP prosthetic foot study [16] and significantly below the 38.15 MPa peak von Mises stress observed in the SACH foot analysis [18], suggesting an enhanced safety margin and a lower risk of localized material failure. Furthermore, in terms of numerical-experimental validation reliability, the present study's maximum deviation of only 4.18% is considerably more accurate than the average error of 15.22% reported in the composite SACH foot modeling and vastly superior to the 30% error margin reported [18] for transtibial prostheses FEA models, thereby demonstrating a highly rigorous methodological accuracy.

B. Validity of Finite Element Analysis

Validation of finite element analysis (FEA) results through mechanical testing showed excellent agreement between the numerical predictions and the experimental results. The deformation difference between the simulation and test results was below 5% across all gait phases: 4.18% at heel strike (HS), 0.81% at mid-stance (MS), and 2.81% at terminal stance (TS). This level of deviation is generally considered indicative of excellent agreement between numerical and experimental results. Previous studies have reported that prediction errors below 5% indicate high model fidelity, whereas deviations below 10% remain acceptable for biomechanical systems involving complex geometries, material behavior, and contact interactions [23][14]. Therefore, the deviations observed in the present study provide strong evidence that the developed finite element model accurately represents the structural response of the proposed SACH foot design. The high consistency between FEA results and experimental testing indicates that the developed numerical model accurately represents the mechanical behavior of the SACH foot prototype. This reflects that the assumptions used in the modeling, including material selection (ABS, HDPE, and vulcanized rubber), boundary conditions, and loading scenarios, have sufficiently represented the real conditions.

Previous studies have emphasized that experimental validation is crucial for ensuring that FEA models are not only mathematically accurate but also physically relevant for prosthetic applications [29]. The biggest difference between the simulation and experimental results occurred in the heel strike phase, which can be attributed to the complexity of the contact interaction between the prosthetic foot and the test surface. In this phase, non-linear phenomena such as local deformation in the elastomer (rubber) and damping are difficult to model perfectly in conventional FEA simulations [35]. In contrast, the smallest deviation occurs during the mid-stance phase, indicating that the loading conditions in this phase are more stable and

Manuscript received 8 May *2026*; Revised 10 June *2026*; Accepted 21 June *2026*; Available online 12 July *2026*
Digital Object Identifier (**DOI**): https://doi.org/10.35882/jeeemi.v8i3.1807

closer to the static assumptions used in the FEA simulation.

In the mid-stance phase, the load distribution tends to be more even and is not dominated by dynamic or transient effects, so numerical models can represent these conditions more accurately. These findings are consistent with previous studies, which show that FEA accuracy improves under more stable and linear loading conditions [34]. In the terminal stance phase, despite a significant increase in deformation, the deviation between the simulation and experimental results remained within a low limit (2.81%). This shows that the FEA model captures the structure's response under maximum load conditions quite well. The terminal stance phase is a critical phase in the gait cycle because it involves peak ground reaction forces and high energy transfer. The accuracy of deformation prediction in this phase is very important as it is directly related to the energy return performance and running efficiency of the prosthesis user [31]. Overall, the high degree of compatibility between FEA results and mechanical testing suggests that the simulation approach used can be relied upon as a prediction tool in the prosthetic design process. This has significant practical implications, as the use of validated FEA can reduce the need for repetitive prototyping, reduce development costs, and accelerate the design innovation process. The integration of numerical simulation and experimental validation is an effective approach to the development of modern engineering-based orthotic and prosthetic devices [36].

However, some limitations remain. First, the FEA model still assumes homogeneous, isotropic materials, whereas in real conditions, materials such as rubber exhibit nonlinear, viscoelastic behavior. Second, the test was conducted under quasi-static conditions, so it did not fully represent the dynamic conditions during walking, including the effects of material fatigue from cyclic loads. Previous studies emphasized the importance of considering fatigue and dynamic load analysis in the long-term evaluation of prosthetic devices [37]. In addition, environmental factors such as temperature and humidity, as well as variations in user gait patterns, have also not been included in the simulation model. Recent research suggests that these factors may affect the mechanical response of polymer and elastomer materials commonly used in prosthetics [38]. Therefore, the development of a more complex FEA model that accounts for these factors is a direction for future research.

C. Comparison Between Polymer and Wooden Keel SACH Foot

The results showed a statistically significant difference in the total deformation value between the polymer keel-based SACH foot prototype and the local SACH foot with a wooden keel in all gait phases. The prototype consistently showed lower deformation than the local design, indicating better mechanical performance in holding loads during the running cycle. These findings confirm that the selection of keel material plays a crucial role in determining the structural response of the prosthetic foot.

Biomechanically, the lower deformation observed in the polymer-keel prototype indicates increased structural stiffness, which is essential for improving load transfer efficiency and gait stability during the stance phase. However, contemporary prosthetic design dictates that performance is not achieved by merely maximizing stiffness, as excessively rigid structures compromise shock absorption and energy return [30][39][40][41]. The proposed polymer-keel design successfully optimizes this balance; while it deforms less than the wooden keel ensuring stability it still operates within a measurable elastic range. The strategic integration of the ABS keel with an HDPE footplate and vulcanized rubber enables the structure to effectively attenuate impact forces. Consequently, the observed deformation profile reflects an improved, controlled load distribution rather than absolute rigidity, supporting both long-term user comfort and mechanical durability without the unpredictable performance variations typical of heterogeneous wooden keels. Recent studies have shown that polymer-based and 3D-printed prosthetic foot can achieve biomechanical performance comparable to or superior to conventional designs [39][40].

In contrast, wooden materials are more susceptible to variability, moisture absorption, and long-term degradation, which may negatively affect performance consistency. The improved mechanical performance observed in the polymer-keel design supports the transition toward polymer-based prosthetic solutions. Despite the promising structural rigidity of Model A, prosthetic foot performance is not determined solely by stiffness. For low-mobility amputees, excessive stiffness may reduce shock absorption, disrupt rollover smoothness, and compromise user comfort. Therefore, while lower deformation ensures stability and structural longevity, future clinical validations encompassing gait symmetry, dynamic plantar pressure, socket comfort, and metabolic energy expenditure are strictly necessary before claiming practical superiority over traditional wooden keels in daily usage scenarios.

Furthermore, several methodological limitations must be acknowledged. The experimental validation in this study relied primarily on global deformation metrics. While this provides a macroscopic validation of the FEA model, incorporating local strain measurements (e.g., using strain gauges or digital image correlation) at critical regions of the keel would substantially strengthen the mechanical validation. Additionally, the evaluation was conducted exclusively under quasi-static loading. Since prosthetic foot

Manuscript received 8 May *2026*; Revised 10 June *2026*; Accepted 21 June *2026*; Available online 12 July *2026*
Digital Object Identifier (**DOI**): https://doi.org/10.35882/jeeemi.v8i3.1807

undergoes repetitive dynamic gait cycles, future research must incorporate cyclic fatigue testing to accurately characterize long-term viscoelastic degradation and the true fatigue life of the polymer materials.

V. Conclusion

This study aimed to design, evaluate, and experimentally validate a polymer-based keel SACH foot as a low-cost alternative, and to assess its mechanical performance relative to a conventional wooden-keel design. Through finite element analysis (FEA), Model A demonstrated the most optimal structural performance among the three configurations, exhibiting the lowest average total deformation (20.12 mm), minimum von Mises stress (12.67 MPa), and the highest factor of safety (1.59). The reliability of the FEA model was successfully validated through static mechanical testing, showing strong agreement with numerical predictions (deviations below 5% across all gait phases: 4.18% at heel strike, 0.81% at mid-stance, and 2.81% at terminal stance). Furthermore, comparative experimental testing revealed that the polymer-keel SACH foot exhibited significantly lower total deformation than the conventional wooden-keel design ($p < 0.05$), indicating superior structural stiffness and more efficient load distribution. Despite these promising results, this study has several limitations that must be addressed in future work. The evaluation was conducted exclusively under quasi-static loading conditions, which does not fully capture the dynamic forces of real amputee gait or evaluate fatigue life under cyclic loading. Additionally, the numerical simulations assumed homogeneous, isotropic, and linearly elastic material properties, and the study did not assess clinical parameters such as user comfort or metabolic energy cost. Future research should integrate dynamic gait simulations with non-linear viscoelastic material models, fatigue testing, and in vivo clinical trials to fully establish the long-term reliability and functional benefits of the proposed polymer-keel SACH foot.

Acknowledgment

The author would like to express his gratitude and high appreciation to Sirindhorn School of Prosthetics and Orthotics, Faculty of Medicine, Siriraj Hospital, Mahidol University, Bangkok, Thailand, Department of Prosthetic and Orthotic, Polytechnic Kesehatan Surakarta, Indonesia, and Department of Mechanical Engineering, Diponegoro University, Indonesia, for the support and facilities in this research. Contributions from all parties in the completion of this work. This study can be realized through a shared commitment to advancing innovation in prosthetics and orthotics.

Funding

This research received no specific grant from any funding agency in the public, commercial, or not-for-profit sectors.

Data Availability

The datasets generated and analyzed during the current study are available from the corresponding author upon reasonable request.

Author Contribution

Agus Setyo Nugroho played a role in conceptualizing and designing research, conducting data collection, and participating in data analysis and interpretation. Kazuhiko Sasaki and Muhammad Nouman contributed to guiding the implementation of the research, monitoring data collection, and writing and revising the manuscript. Rifky Ismail assisted in the implementation of the research and provided critical feedback on the manuscript. All authors reviewed and approved the final version of the manuscript and agreed to be responsible for all aspects of the work that ensure integrity and accuracy.

Declarations

Ethical Approval

No human participants or patient data were involved in this study. Institutional review board approval was obtained as part of the broader prosthetics research program conducted at the institution. This research was conducted in accordance with ethical standards and has received approval from the Institutional Ethics Agency (IRB) of the Politeknik Kesehatan Surakarta, Indonesia, with approval number DP.04.04/F.XXV/2959/2024.

Consent for Publication Participants.

Consent for publication not applicable

Competing Interests

The authors declare no competing interests.

References

[1] World Health Organization, *Global report on assistive technology*. World Health Organization, 2022.

[2] B. J. Hafner, E. G. Halsne, S. J. Morgan, D. C. Morgenroth, and A. T. Humbert, “Effects of prosthetic foot on metabolic energy expenditure in people with transtibial amputation: A systematic review and meta-analysis.,” *PM R*, vol. 14, no. 9, pp. 1099–1115, Sep. 2022, doi: 10.1002/pmrj.12693.

[3] K. Alluhydan, M. I. H. Siddiqui, and H. Elkanani, “Functionality and Comfort Design of Lower-Limb Prosthetics: A Review,” *Journal of*

Manuscript received 8 May *2026*; Revised 10 June *2026*; Accepted 21 June *2026*; Available online 12 July *2026*
Digital Object Identifier (**DOI**): https://doi.org/10.35882/jeeemi.v8i3.1807

Disability Research, vol. 2, no. 3, Sep. 2023, doi: 10.57197/JDR-2023-0031.

[4] T. Mannan Balaramakrishnan, S. Natarajan, and S. Sujatha, "Design of a biomimetic sach foot: An experimentally verified finite element approach," *Journal of Biomimetics, Biomaterials and Biomedical Engineering*, vol. 45, pp. 22–30, 2020, doi: 10.4028/www.scientific.net/jbbbe.45.22.

[5] M. Falbriard *et al.*, "A functional approach towards the design, development, and test of an affordable dynamic prosthetic foot," *PLoS One*, vol. 17, no. 5, p. e0266656, May 2022.

[6] F. M. Kadhim, S. A. Fadhil, A. M. Abdullah, and M. S. Al-Din Tahir, "Designing and manufacturing a flexible heel of a printed prosthetic foot for rehabilitation," *International Review of Applied Sciences and Engineering*, vol. 16, no. 2, pp. 324–330, Jun. 2025, doi: 10.1556/1848.2024.00930.

[7] H. A. Abdalwahhab and K. K. Resan, "Development and mechanical analysis of a novel prosthetic foot with a flexible keel for improved functionality," in *The International Middle Eastern Simulation and Modelling Conference, MESM 2023*, 2024, pp. 71–75.

[8] H. A. Abdalwahhab, K. K. Resan, and E. Omaraa, "Comparing Maximum Lifespan of a New Flexible Keel versus Non-Articulated Prosthetic Foot," *Journal of Engineering and Sustainable Development*, vol. 29, no. 1, pp. 89–95, 2025, doi: 10.31272/jeasd.2193.

[9] A. P. Usman and S. Sugiri, "Analysis of the strength of timber and glulam timber beams with steel reinforcement," *Journal of Engineering and Technological Sciences*, vol. 47, no. 6, pp. 601–611, 2015, doi: 10.5614/j.eng.technol.sci.2015.47.6.1.

[10] S. L. Sashenkov, A. N. Panasenko, A. A. Episheva, F. V Merkulyev, Y. V Burnashov, and A. A. Piskaev, "Analysis of opportunities for the development of a brand-new prothetic foot," *Human Sport Medicine*, vol. 23, no. 4, pp. 155–162, 2023, doi: 10.14529/hsm230419.

[11] M. Broda, P. Kryg, and G. A. Ormondroyd, "Gap-fillers for wooden artefacts exposed outdoors—a review," *Forests*, vol. 12, no. 5, 2021, doi: 10.3390/f12050606.

[12] E. N. Abbas, K. K. Resan, M. J. Jweeg, E. K. Njim, and R. Madan, "Fabrication and experimental analysis of a novel flexible keel prosthetic foot utilizing functionally graded materials," *J. Med. Eng. Technol.*, pp. 1–9, doi: 10.1080/03091902.2025.2570158.

[13] P. Chauhan, A. K. Singh, and N. K. Raghuwanshi, "The state of art review on prosthetic foot and its significance to imitate the biomechanics of human ankle-foot," *Mater. Today Proc.*, vol. 62, pp. 6364–6370, 2022, doi: 10.1016/j.matpr.2022.03.379.

[14] N. Worajinda, J. Phromjan, R. Rugsaj, S. Phakdee, and C. Suvanjumrat, "Design and Analysis of a Composite SACH Foot: Experimental Validation and Finite Element Modeling," *Key Eng. Mater.*, vol. 1016, pp. 115–120, 2025, doi: 10.4028/p-6LrQlL.

[15] G. Barrera *et al.*, "The Effect of Surface Treatments on the Mechanical Properties of Low-Density Polyethylene/Natural Rubber Composites Reinforced with Sugarcane Bagasse Ash," *Journal of Composites Science*, vol. 9, no. 9, 2025, doi: 10.3390/jcs9090489.

[16] P. Maroti *et al.*, "Additive manufacturing in limb prosthetics and orthotics: the past, present and future of 3D printing orthopedic assistive devices," in *Medical Additive Manufacturing*, Elsevier, 2024, pp. 179–207. doi: 10.1016/B978-0-323-95383-2.00028-7.

[17] V. Plesec, J. Humar, P. Dobnik-Dubrovski, and G. Harih, "Numerical Analysis of a Transtibial Prosthesis Socket Using 3D-Printed Bio-Based PLA," *Materials*, vol. 16, no. 5, p. 1985, Feb. 2023, doi: 10.3390/ma16051985.

[18] E. Pelita, T. R. Hidayani, and A. Akbar, "Analysis physical properties of composites polymer from cocofiber and polypropylene plastic waste with maleic anhydrate as crosslinking agent," in *IOP Conference Series: Materials Science and Engineering*, 2017. doi: 10.1088/1757-899X/223/1/012060.

[19] L. Indrie, S. McNeil, M. M. Mutlu, S. Bota, D. C. Ilieș, and H. A. Karavana, "The Initial Development and Evaluation of Cross-Linked Casein Films for Sustainable Footwear," *Coatings*, vol. 13, no. 2, 2023, doi: 10.3390/coatings13020217.

[20] S. G. Nukala, I. Kong, A. B. Kakarla, V. I. Patel, and H. Abuel-Naga, "Simulation of Wood Polymer Composites with Finite Element Analysis," *Polymers (Basel).*, vol. 15, no. 9, 2023, doi: 10.3390/polym15091977.

[21] A. Vasanthanathan, S. M. Kennedy, K. Amudhan, K. Jairooban, S. Karthikeyan, and B. Vignesh, "Design, optimization, FEA and fabrication of lightweight CFRP prosthetic foot," *Progress in Engineering Science*, vol. 3, no. 1, 2026, doi: 10.1016/j.pes.2025.100200.

[22] M. Omasta, D. Paloušek, T. Návrat, and J. Rosický, "Finite element analysis for the evaluation of the structural behaviour, of a prosthesis for trans-tibial amputees," *Med. Eng. Phys.*, vol. 34, no. 1, pp. 38–45, 2012, doi: 10.1016/j.medengphy.2011.06.014.

Manuscript received 8 May *2026*; Revised 10 June *2026*; Accepted 21 June *2026*; Available online 12 July *2026*
Digital Object Identifier (**DOI**): https://doi.org/10.35882/jeeemi.v8i3.1807

[23] T. Mannan Balaramakrishnan, S. Natarajan, and S. Sujatha, "Energy storage and stress–strain characteristics of a prosthetic foot: a priori design and analysis with experiments," *Int. J. Numer. Method. Biomed. Eng.*, vol. 38, no. 4, p. e3579, Apr. 2022, doi: https://doi.org/10.1002/cnm.3579.

[24] J. P. M. Tribst, A. M. O. Dal Piva, M. A. Bottino, R. S. Nishioka, A. L. S. Borges, and M. Özcan, "Digital Image Correlation and Finite Element Analysis of Bone Strain Generated by Implant-Retained Cantilever Fixed Prosthesis," *European Journal of Prosthodontics and Restorative Dentistry*, vol. 28, no. 1, pp. 10–17, 2020, doi: 10.1922/EJPRD_1941Tribst08.

[25] N. N. Subhash *et al.*, "Structural Performance Assessment of FUPRO Grace Foot.," *Trends Biomater. Artif. Organs*, vol. 36, no. 2, 2022.

[26] K. Shah and M. U. Rehman, "Finite Element Analysis of Custom Designed and Additive Manufactured Total Surface Bearing Prosthesis for Trans-Tibial Amputees," *Applied Sciences*, vol. 15, no. 3, p. 1284, Jan. 2025, doi: 10.3390/app15031284.

[27] L. Baldassari, M. Minuto, E. Gruppioni, and M. Frascio, "Design, Testing and Validation of a Cost Effective and Sustainable Bamboo Prosthetic Foot," *Prosthesis*, vol. 7, no. 5, p. 124, Oct. 2025, doi: 10.3390/prosthesis7050124.

[28] A. R. N. Al Thahabi, L. M. Martulli, A. Sorrentino, M. Lavorgna, E. Gruppioni, and A. Bernasconi, "Stiffness-driven design and optimization of a 3D-printed composite prosthetic foot: A beam finite Element-Based framework," *Compos. Struct.*, vol. 337, p. 118053, Jun. 2024, doi: 10.1016/j.compstruct.2024.118053.

[29] T. M. Balaramakrishnan, S. Natarajan, and S. Sujatha, "Biomechanical design framework for prosthetic foot: Experimentally validated non-linear finite element procedure," *Med. Eng. Phys.*, vol. 92, pp. 64–70, 2021, doi: https://doi.org/10.1016/j.medengphy.2021.04.006.

[30] E. G. Halsne, J. M. Czerniecki, J. B. Shofer, and D. C. Morgenroth, "The effect of prosthetic foot stiffness on foot-ankle biomechanics and relative foot stiffness perception in people with transtibial amputation," *Clinical Biomechanics*, vol. 80, Dec. 2020, doi: 10.1016/j.clinbiomech.2020.105141.

[31] A. K. Faizin, N. Adyono, W. D. Lestari, A. A. Yusuf, and M. I. Ammarullah, "A novel prosthetic foot with a flexible rubber ankle for the Indonesian population: a finite element analysis," *BMC Musculoskelet. Disord.*, vol. 26, no. 1, p. 1119, Dec. 2025, doi: 10.1186/s12891-025-09418-w.

[32] F. Tavangarian, N. K. Khairunajhan, M. S. M. Yusairi, L. H. I. Nasir, F. H. Mazlan, and A. Attaluri, "3D printed pylon for lower limb prosthetic device inspired by spicule architecture," *Exploration of BioMat-X*, vol. 2, Sep. 2025, doi: 10.37349/ebmx.2025.101347.

[33] W. D. L. Lestari, Y. Ariadi, and A. Putra, "Customized Prosthetic Foot via Topology Optimization and 3D Printing: A Critical Review," *Advanced Mechanical and Mechatronic Systems*, vol. 2, no. 1, pp. 33–49, Dec. 2025, doi: 10.53623/amms.v2i1.776.

[34] C.-H. Yeh, K.-R. Lin, F.-C. Su, H.-Y. Hsu, L.-C. Kuo, and C.-C. Lin, "Optimizing 3D printed ankle-foot orthoses for patients with stroke: Importance of effective elastic modulus and finite element simulation," *Heliyon*, vol. 10, no. 5, p. e26926, Mar. 2024, doi: 10.1016/j.heliyon.2024.e26926.

[35] R. B. Al-Tameemi, H. Mazaheri, J. S. Chiad, and M. Shaban, "Biomechanical Comparison of SACH, Single-Axis, and Multi-Axis Prosthetic Foot with Osseointegrated Implants Using Ground Reaction Force.," *Int. J. Adv. Sci. Eng. Inf. Technol.*, vol. 16, no. 2, p. 353, 2026.

[36] M. Abas, T. Habib, and S. Noor, "Design and analysis of solid ankle foot orthosis by employing mechanical characterization and a low-cost scanning approach for additive manufacturing," *Rapid Prototyp. J.*, vol. 30, no. 4, pp. 782–797, Apr. 2024, doi: 10.1108/RPJ-09-2023-0316.

[37] D. Trindade *et al.*, "Material Performance Evaluation for Customized Orthoses: Compression, Flexural, and Tensile Tests Combined with Finite Element Analysis," *Polymers (Basel).*, vol. 16, no. 18, p. 2553, Sep. 2024, doi: 10.3390/polym16182553.

[38] N. B. Mohammed and Y. Y. Kahtan, "Developmental study of a 3D prosthetic foot using finite element analysis," *International Journal of Advanced Technology and Engineering Exploration*, vol. 11, no. 120, p. 1592, 2024, doi: 10.19101/IJATEE.2024.111100971.

[39] U. Trinler, D. W. W. Heitzmann, S. Hitzeroth, M. Alimusaj, M. Rehg, and A. Hogan, "Biomechanical comparison of a 3D-printed prosthetic foot with conventional foot in people with transtibial amputation: A prospective cohort study," *Prosthet. Orthot. Int.*, vol. 47, no. 1, 2023.

[40] S. Bhatt, D. Joshi, P. K. Rakesh, and A. K. Godiyal, "Advances in additive manufacturing processes and their use for the fabrication of lower limb prosthetic devices," *Expert Rev. Med. Devices*, vol. 20, no. 1, pp. 17–27, Jan. 2023, doi: 10.1080/17434440.2023.2169130.

[41] A. Kurakin, A. Sergeev, D. Korostovskaya, A. Kurenkova, and V. Serdyukov, "Development

Manuscript received 8 May *2026*; Revised 10 June *2026*; Accepted 21 June *2026*; Available online 12 July *2026*
Digital Object Identifier (**DOI**): https://doi.org/10.35882/jeeemi.v8i3.1807

and Comprehensive Evaluation of 3D-Printed Prosthetic Foot: Modeling, Testing and a Pilot Gait Study," *Prosthesis*, vol. 8, no. 4, p. 40, Apr. 2026, doi: 10.3390/prosthesis8040040.

Author Biography

Agus Setyo Nugroho. He obtained an Applied Bachelor of Prosthetic and Orthotic from the Politeknik Kesehatan Kemenkes Surakarta in 2013, an M. Kes. in the field of Family Medicine from Sebelas Maret University Surakarta, Indonesia in 2014, and since 2022, has been pursuing a Ph.D Prosthetic and Orthotic from Faculty of Medicine, Siriraj Hospital, Mahidol University, Bangkok, Thailand. Since 2010, he has been serving as a Lecturer in the Department of Prosthetic and Orthotics at Politeknik Kesehatan Surakarta, Indonesia. His current research interests include the development of affordable lower limb prosthetic innovations for developing countries.

Kazuhiko Sasaki. He has been an Assistant Professor at the Faculty of Medicine, Siriraj Hospital, Mahidol University, Thailand, since 2018. He received a Bachelor of Science in Physics from Tokyo University of Science in Japan in 1999. He received a Master of Engineering Bio-Applications and Systems Engineering in March 2002 from Tokyo University of Agriculture and Technology, Japan. And a Ph.D Engineering in Electronic and Information Engineering on June 29, 2005, from Tokyo University of Agriculture and Technology, Japan. He has worked at the Sirindhorn School of Prosthetics and Orthotics, Faculty of Medicine, Siriraj Hospital, Mahidol University, Bangkok, Thailand, from 2011 to the present.

Muhammad Nouman. He received a Bachelor of Prosthetics and Orthotics in 2014 from Sirindhorn School of Prosthetics and Orthotics, Faculty of Medicine, Siriraj Hospital, Mahidol University, Bangkok, Thailand. In March 2017, he received an M.Sc. in Biomedical Engineering from the Institute of Biomedical Engineering, Faculty of Medicine, Prince of Songkla University, Hat Yai, Songkhla, Thailand, and in April 2021, he received a Ph.D Biomedical Engineering, Institute of Biomedical Engineering, Faculty of Medicine, Prince of Songkla University, Hat Yai, Songkhla, Thailand. Since 2021, he has been serving as a Lecturer at the Sirindhorn School of Prosthetics and Orthotics, Faculty of Medicine Siriraj Hospital, Mahidol University, Bangkok, Thailand.

Rifky Ismail. He is a Professor and Head of the Bachelor Program of Mechanical Engineering at Diponegoro University, Semarang, Indonesia. He obtained his Bachelor of Engineering degree in 2003 from the Department of Mechanical Engineering, Diponegoro University. He earned his Master of Engineering in 2007 from the Department of Mechanical and Industrial Engineering at Gajah Mada University, Yogyakarta, Indonesia. In 2013, he earned a Doctor of Engineering degree from the Department of Mechanical Engineering at the University of Twente, the Netherlands. He is also active in research and development in prosthetics and orthotics through the Center of Excellence (COE) for Health Technology, CBIOM3S, UNDIP.

Manuscript received 8 May *2026*; Revised 10 June *2026*; Accepted 21 June *2026*; Available online 12 July *2026*
Digital Object Identifier (**DOI**): https://doi.org/10.35882/jeeemi.v8i3.1807